# A Study on Correlations Between the Initial Optical and Scintillation Properties and Their Radiation Damage for Lead Tungstate Crystals

Jianming Chen, *Member, IEEE*, Rihua Mao, Liyuan Zhang, *Member, IEEE*, and Ren-yuan Zhu, *Senior Member, IEEE*

***Abstract*—This paper presents a study of correlations between the initial optical and scintillation properties and their radiation damage for mass produced lead tungstate crystals. A correlation was observed between crystal's initial light outputs and the values of its initial longitudinal transmittance at 360 nm. A strong correlation was found between the emission weighted radiation induced absorption coefficients and the relative losses of the longitudinal transmittance at 440 nm. Correlations were also observed between the relative losses of crystal's light output and the relative losses of its longitudinal transmittance at 440 nm, or the emission weighted radiation induced absorption coefficients. No correlations were observed between crystal's radiation hardness and its initial longitudinal transmittance or the slope of the initial longitudinal transmittance across the band edge.**

***Index Terms*—Lead tungstate, light output, radiation damage, transmittance.**

## I. Introduction

LEAD tungstate ($PbWO_4$ or PWO) is a heavy crystal scintillator with a high density (8.3 g/cm$^3$), a short radiation length (0.89 cm) and a small Molière radius (2.2 cm). Yttrium doped $PbWO_4$ crystals have an emission spectrum peaked at 420 nm with a FWHM of 120 nm [1]. After extensive R&D, $PbWO_4$ crystals are now in mass production. As of this writing more than fifty thousands crystals have been produced at Bogoroditsk Techno-Chemical Plant (BTCP) in Tula, Russia, for the CMS experiment at CERN [2]. Shanghai Institute of Ceramics (SIC) in Shanghai, China, has also produced several thousand crystals for the PrimEx experiment at Jefferson laboratory [3] as well as for the CMS experiment. Following our previous studies [4], we present in this paper a study on correlations between the initial optical and scintillation properties and their radiation damage for mass produced lead tungstate crystals.

A total of 53 $PbWO_4$ samples were studied: 21 from BTCP and 32 from SIC. All 21 BTCP samples are of the CMS endcap size with a slightly tapered shape: $30 \times 30$ mm$^2$ at the large end, $28.5 \times 28.5$ mm$^2$ at the small end and 220 mm long. Among the 32 samples from SIC, 20 samples have a rectangular shape of $22 \times 22 \times 230$ mm$^3$, and the other 12 are of the CMS endcap size. All surfaces of these samples are polished. It is interesting to note that the BTCP $PbWO_4$ crystals are triple doped with lanthanum, yttrium and niobium [5], and are grown along the "$a$" axis by the Czochralski method. SIC $PbWO_4$ crystals, however, are single doped with yttrium only and are grown along the "$c$" axis by the modified Bridgman method [4].

All samples were first annealed at 200°C for 4 hours to remove any residual radiation induced absorption and to restore the sample to its initial state [6], [7]. The annealing temperature was chosen to be effective in removing radiation induced effect based upon our experience obtained in previous studies on scintillating crystals [8]. After annealing, all samples were kept in the dark at 18°C for at least 48 hours before the initial measurements. It was found that $PbWO_4$ crystal's optical and scintillation properties are stabilized 8 hours after the completion of the thermal annealing [9]. After the initial measurements, all samples went through a series of $\gamma$-ray irradiations at the dose rates of 15, 100, 400 and 9 000 rad/h until reaching an equilibrium [8]. Optical and scintillation properties were also measured after each step of the irradiations.

## II. Optical and Scintillation Properties

### A. Light Output

The blue scintillation of the yttrium doped $PbWO_4$ crystals have a fast decay time. The scintillation light output and decay kinetics were measured by using a Hamamatsu PMT R2059 with a bialkali photo cathode and a quartz window. For measurements of the light output the large end of the sample was coupled to the PMT with Dow Corning 200 fluid, while all other faces of the sample were wrapped with the Tyvek paper. A collimated $^{137}$Cs source was used to excite the sample. The $\gamma$-ray peak positions were obtained by a simple Gaussian fit, and were used to determine photoelectron numbers by using calibrations of the single photo electron peak. The measured light output values were corrected to that of 18°C by using corresponding temperature coefficient. The light output of a sample is defined as an average of 9 data points obtained by shooting the $\gamma$-ray source at 9 evenly distributed locations along the long crystal side. The systematic uncertainty of light output measurement thus was reduced to less than 1% [1].

### B. Longitudinal Transmittance

The longitudinal transmittance was measured by using a Hitachi U-3210 UV/visible spectrophotometer with double beam, double monochromator and a large sample compartment equipped with a custom Halon PTFE coated integrating sphere.

Manuscript received October 13, 2006; revised January 9, 2007. This work was supported in part by the U.S. Department of Energy Grant DE-FG03-92-ER40701.

The authors are with the California Institute of Technology, Pasadena, CA 91125 USA (e-mail: zhu@hep.caltech.edu).

Color versions of one or more of the figures in this paper are available online at http://ieeexplore.ieee.org.

Digital Object Identifier 10.1109/TNS.2007.891673

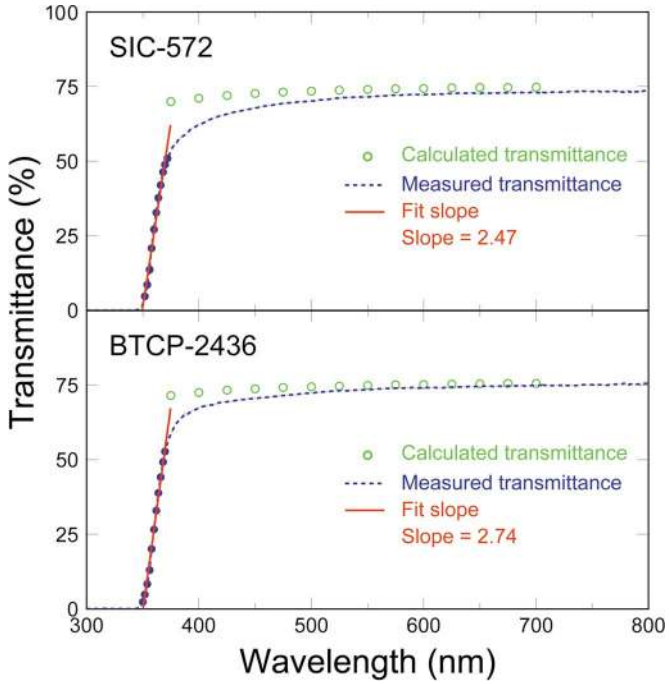


Fig. 1. The longitudinal transmittance spectra (dashed lines) for the samples SIC-572 (top) and BTCP-2436 (bottom) are shown as function of wavelength. Also shown in the figure are the theoretical limit (open circles), calculated according to the (1), and the data points (solid dots) used for the linear fits to obtain the slopes across the bank edge.

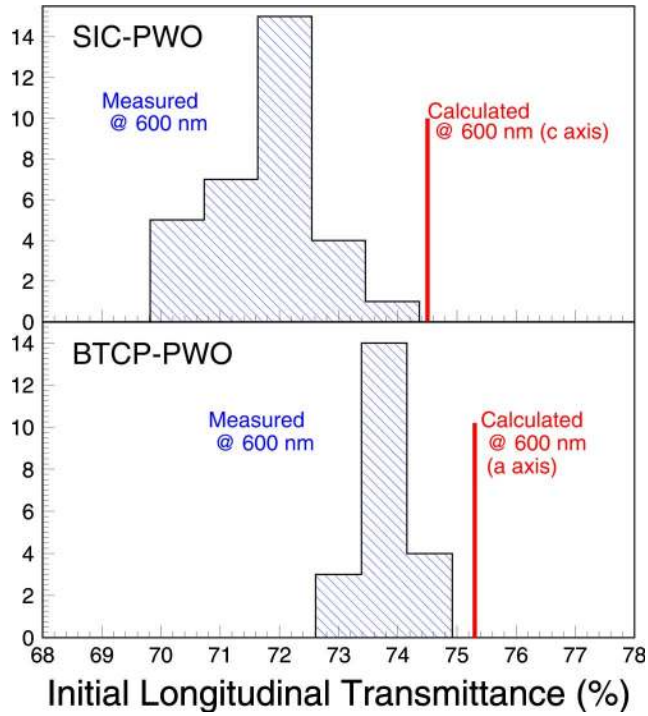


Fig. 2. The longitudinal transmittance values measured at 600 nm for all SIC (top) and BTCP (bottom) samples are compared to the theoretical limit calculated according to the (1).

The systematic uncertainty in repeated measurements was about 0.25%. Fig. 1 shows the measured longitudinal transmittance spectra for the samples SIC-572 (top) and BTCP-2436 (bottom). The measured transmittance spectra are compared to the theoretical limit of transmittance, $T_s$ (open circles in Fig. 1), which was calculated by using corresponding refractive indices assuming no internal absorption [10] following

$$T_s = (1-R)^2 + R^2(1-R)^2 + \cdots = \frac{(1-R)}{(1+R)}, \qquad (1)$$

where

$$R = \frac{(n_{\text{crystal}} - n_{\text{air}})^2}{(n_{\text{crystal}} + n_{\text{air}})^2}. \qquad (2)$$

A comparison of the measured initial longitudinal transmittance and the $T_s$ may reveal crystal's preexisting internal absorption and internal scattering. Fig. 2 shows a comparison of the longitudinal transmittance values measured at 600 nm for all SIC (top) and BTCP (bottom) samples. Also shown in this figure are the theoretical limits of the longitudinal transmittance calculated according to the (1). An attention was paid to the birefringent nature of the $PbWO_4$ crystals [11] in such comparison. Since the BTCP and SIC samples were grown along the "$a$" and "$c$" axis respectively their corresponding theoretical limit for the longitudinal transmittance must be calculated by using the refractive indices of the "extraordinary" and the "ordinary" light respectively. The resultant theoretical transmittance limit of the "extraordinary" light is about 3% higher than that of the "ordinary" light at the $PbWO_4$ emission peak: 420 nm. In this calculation and our early calculation [6] the numerical values of the PWO refractive indices for the "extraordinary" and the "ordinary" light are obtained from the [11], which was confirmed by a later measurement [12]. As shown in Fig. 1 and 2 both BTCP and SIC samples approach the theoretical limit at long wavelengths, indicating very low preexisting absorption and internal scattering. The SIC samples show a wide distribution partly because the samples have two different lengths: 22 cm and 23 cm.

### C. Slope of the Longitudinal Transmittance Across the Band Edge

Also shown in Fig. 1 are the slope values of the longitudinal transmittance across the band edge. They were obtained by using a linear fit (straight lines) to 10 longitudinal transmittance data points (black dots) measured between two wavelengths: $\lambda_a$ and $\lambda_b$. Because of $PbWO_4$ crystal's birefringent nature, the values of $\lambda_a$ and $\lambda_b$ are also axis orientation dependent, and thus crystal vendor dependent. They are 350 nm and 370 nm respectively for the BTCP samples, and are 352 nm and 372 nm respectively for the SIC samples.

### D. Dose Rate Dependent Damage in Transmittance

$PbWO_4$ crystals are known to suffer from radiation damage caused by the formation of the radiation induced color centers [8]. Although there is no damage to the scintillation mechanism, these radiation induced color centers would absorb scintillation light, and thus reduce crystal's light output. It is also known that radiation induced color centers may annihilate at the room temperature. During irradiations, both annihilation and creation

processes coexist. Assuming that the annihilation speed of the color center $i$ is proportional to a constant $a_i$ and its creation speed is proportional to a constant $b_i$ and the dose rate $(R)$, the differential variation of the color center density when both processes coexist can be written as [8]

$$dD = \sum_{i=1}^{n} \{-a_i D_i + (D_i^{\text{all}} - D_i) b_i R\} dt, \tag{3}$$

where $D_i$ is the density of the color center $i$ in the crystal and the summation goes through all centers. The solution of the (3) is

$$D = \sum_{i=1}^{n} \{\frac{b_i R D_i^{\text{all}}}{a_i + b_i R}[1 - e^{-(a_i + b_i R)t}] + D_i^0 e^{-(a_i + b_i R)t}\}, \tag{4}$$

where $D_i^{\text{all}}$ is the total density of the traps related to the center $i$ and $D_i^0$ is its initial density. This solution shows that the color center density varies as an exponential function. It reaches an equilibrium after about 4.6 times corresponding time constants. After that the effect caused by additional irradiation would be less than 1% if the irradiation condition (dose rate) is kept at the same level. The damage level thus is dose rate dependent, not cumulated dosage dependent. The color center density in the equilibrium $(D_{\text{eq}})$ depends on the dose rate $(R)$ applied:

$$D_{\text{eq}} = \sum_{i=1}^{n} \frac{b_i R D_i^{\text{all}}}{a_i + b_i R}. \tag{5}$$

Figs. 3 and 4 show longitudinal transmittance spectra as a function of wavelength measured before and after a series of irradiations for the samples BTCP-2455 and SIC-U517 respectively. The curves in each plot, in order from top to bottom, represent the longitudinal transmittance spectra measured before irradiations and after the samples reaching an equilibrium at dose rates of 15, 400 and 9 000 rad/h respectively.

### *E. Emission Weighted Radiation Induced Absorption Coefficient*

The radiation induced absorption coefficient and the emission weighted radiation induced absorption coefficient (EWRIAC) [4] can be extracted from the longitudinal transmittance data measured before and after irradiations. The EWRIAC is a measure of the radiation damage, which is defined as

$$rmEWRIAC = \frac{\int Riac(\lambda) Em(\lambda) d\lambda}{\int Em(\lambda) d\lambda}, \tag{6}$$

where the $\text{Riac}(\lambda)$ is the radiation induced absorption coefficient or the overall color center density, and $Em(\lambda)$ is the scintillation emission as a function of wavelength. The inverse of the EWRIAC can be seen as the degraded light attenuation length (LAL). The radiation induced absorption coefficient (Riac), or the color center density, were calculated according to the following equation:

$$\text{Riac} = 1/\text{LAL}_{\text{equilibrium}} - 1/\text{LAL}_{\text{before}}, \tag{7}$$

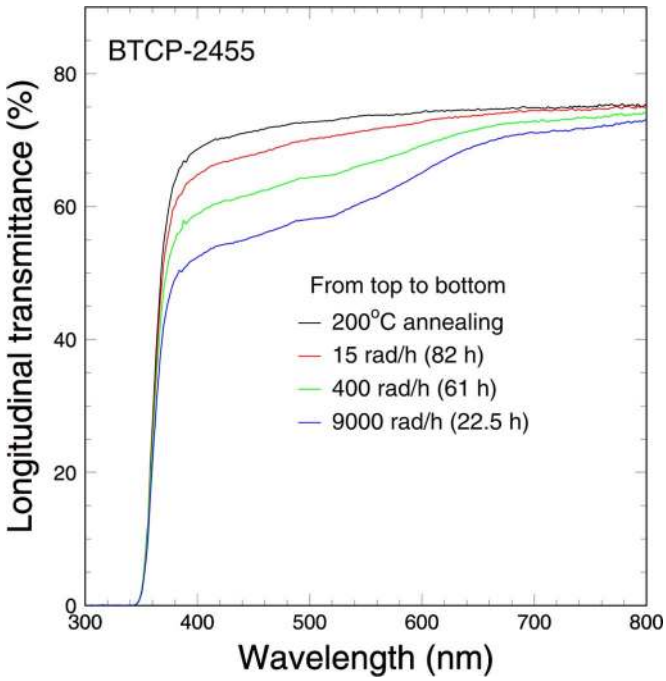


Fig. 3. The longitudinal transmittance spectra measured before irradiations and in the equilibrium under irradiations with dose rates of 15, 400, and 9 000 rad/h are shown as a function of wavelength for the sample BTCP-2455.

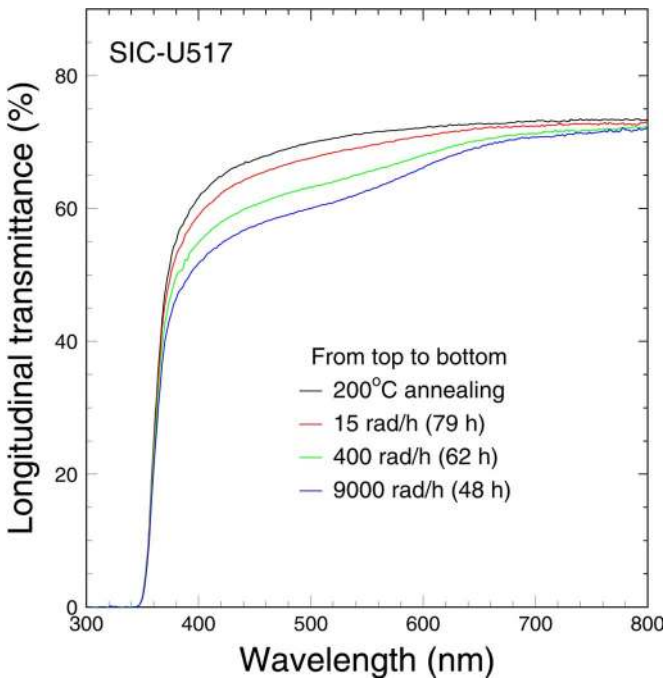


Fig. 4. The longitudinal transmittance spectra measured before irradiations and in the equilibrium under irradiations with dose rates of 15, 400, and 9 000 rad/h are shown as a function of wavelength for the sample SIC-U517.

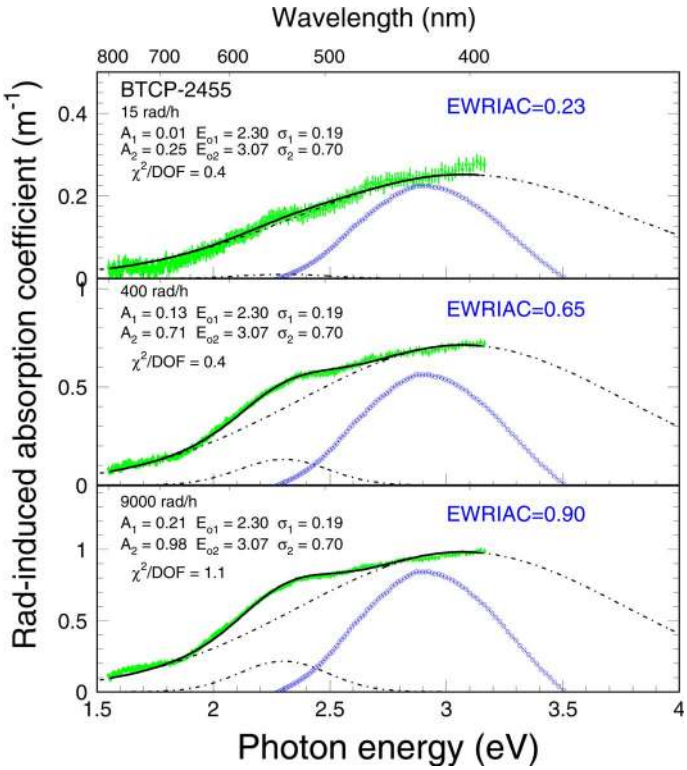


Fig. 5. Radiation induced absorption coefficients (data points with error bars), or color center densities, are shown as a function of the photon energy for the sample BTCP-2455 in the equilibrium under irradiations with dose rate of 15, 400, and 9 000 rad/h irradiations. Also shown in the figure are the emission spectrum (open circles), the decomposed color centers (dot-dashed lines) and the EWRIAC values in units of $m^{-1}$.

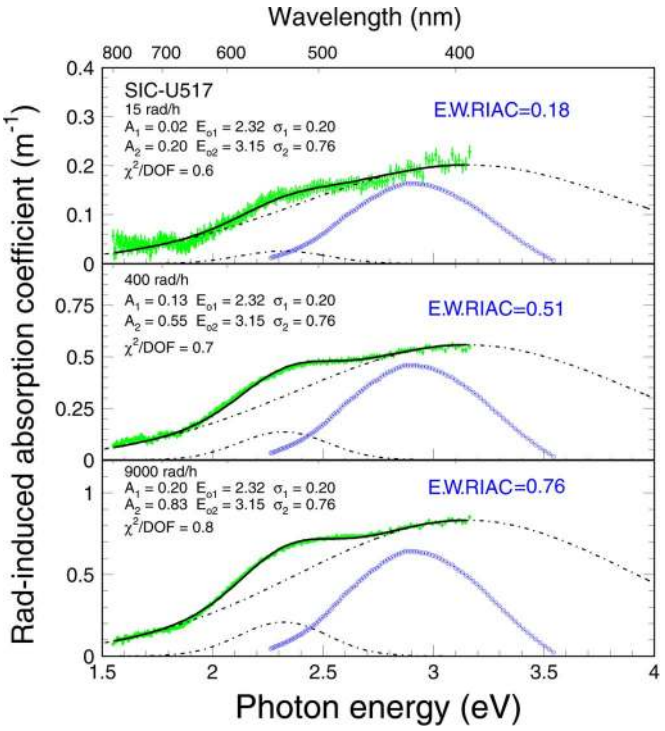


Fig. 6. Radiation induced absorption coefficients (data points with error bars), or color center densities, are shown as a function of the photon energy for the sample SIC-U517 in the equilibrium under irradiations with dose rate of 15, 400, and 9 000 rad/h irradiations. Also shown in the figure are the emission spectrum (open circles), the decomposed color centers (dot-dashed lines) and the EWRIAC values in units of $m^{-1}$.

where the subscripts "equilibrium" and "before" refer to "in equilibrium" and "before irradiation" respectively. The light attenuation length $(LAL)$ was calculated by using the longitudinal transmittance data according to

$$\mathrm{LAL} = \frac{\ell}{\ln\{[T(1-T_s)^2]/[\sqrt{4T_s^4 + T^2(1-T_s^2)^2} - 2T_s^2]\}}, \tag{8}$$

where $T$ is the transmittance measured along crystal length $\ell$ and $T_s$ is the theoretical transmittance without internal absorption defined in the (1).

Figs. 5 and 6 show the measured radiation induced absorption coefficients, or the color center densities, (data points with error bars) as a function of the photon energy for the samples BTCP-2455 and SIC-U517 respectively in the equilibrium under irradiations at the dose rates of 15, 400 and 9 000 rad/h. Also shown in these two figures are the emission spectra (open circles) and the corresponding EWRIAC values calculated according to the (6). In these figures the radiation induced color center densities were decomposed to a sum (solid lines) of two Gaussian shaped color centers (dashed lines):

$$\mathrm{Riac} = \sum_{i=1}^{2} A_i e^{-\frac{(E-E_i)^2}{2\sigma_i^2}} \tag{9}$$

where $E_i$, $\sigma_i$ and $A_i$ denote the energy, width and amplitude of the color center $i$, and $E$ is the photon energy. Attempt of fits with more than two color centers yielded a poorer $\chi^2$ per degree of freedom.

The fits with unified color center peaks and widths for crystals from each vendor provide a good description of the data. The peak/width of these two color centers are 2.30 eV/0.19 eV and 3.07 eV/0.70 eV for all BTCP samples, and are 2.32 eV/0.20 eV and 3.15 eV/0.76 eV for all SIC samples. We observe that the peaks of these two color centers are located at two sides of the $PbWO_4$ crystal's emission peak (2.95 eV). As discussed in the [13], this leads to the choice of 440 nm as the monitoring wavelength for the CMS ECAL. The color centers in the SIC samples are relatively deeper as compared to the BTCP samples. This result is consistent with the observation that the SIC samples have a relatively longer recovery time constants and a shorter damage time constant at high dose rates [14].

Figs. 7 and 8 show distributions of the EWRIAC values as a function of the $\gamma$-ray dose rate for the BTCP and SIC samples respectively. The EWRIAC values of all samples are less than 1 $m^{-1}$ up to 400 rad/h, indicating no damage to the light response uniformity [8] for $PbWO_4$ crystals used in the CMS ECAL barrel, where the maximum dose rate is expected to be a few hundreds rad/h even if the LHC luminosity is increased by a factor of ten (SLHC). The EWRIAC values measured at 9 000 rad/h, however, are diverse. Some samples show up to 3 $m^{-1}$, indicating possible damages in the light response uniformity and thus the energy resolution [8]. Rigorous quality control on radiation hardness thus is required for $PbWO_4$ crystals used in the CMS endcaps.

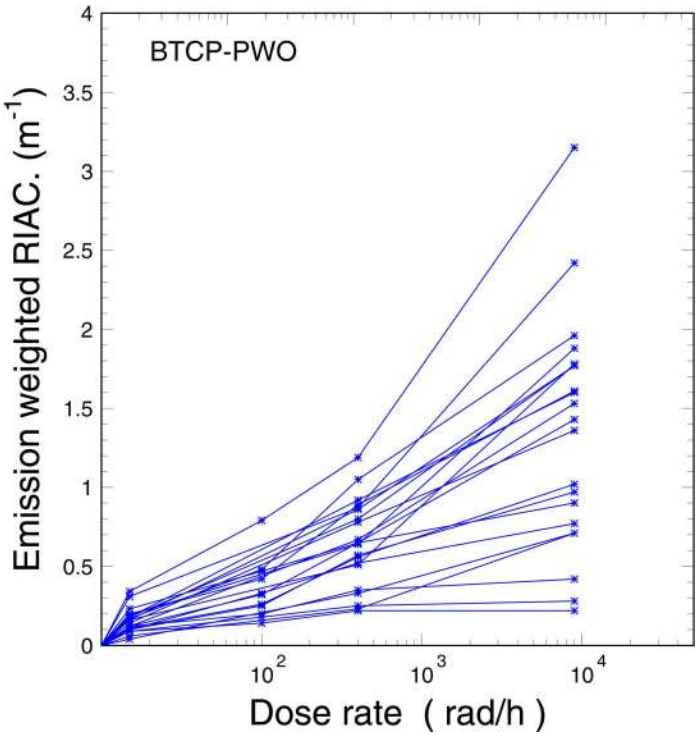


Fig. 7. The EWRIAC values are shown as a function of the dose rate for all BTCP samples in the equilibrium under irradiations with dose rate of 15, 100, 400, and 9 000 rad/h irradiations.

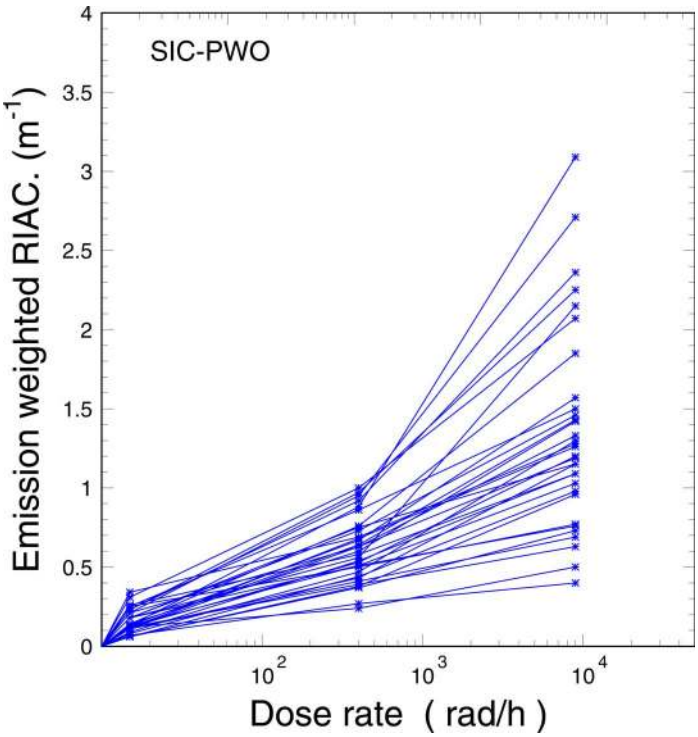


Fig. 8. The EWRIAC values are shown as a function of the dose rate for all SIC samples in the equilibrium under irradiations with dose rate of 15, 400, and 9 000 rad/h irradiations.

## III. Correlations

### A. Initial Light Output Versus Initial Longitudinal Transmittance

Fig. 9 shows correlations between the numerical values of the initial light output and the initial longitudinal transmission

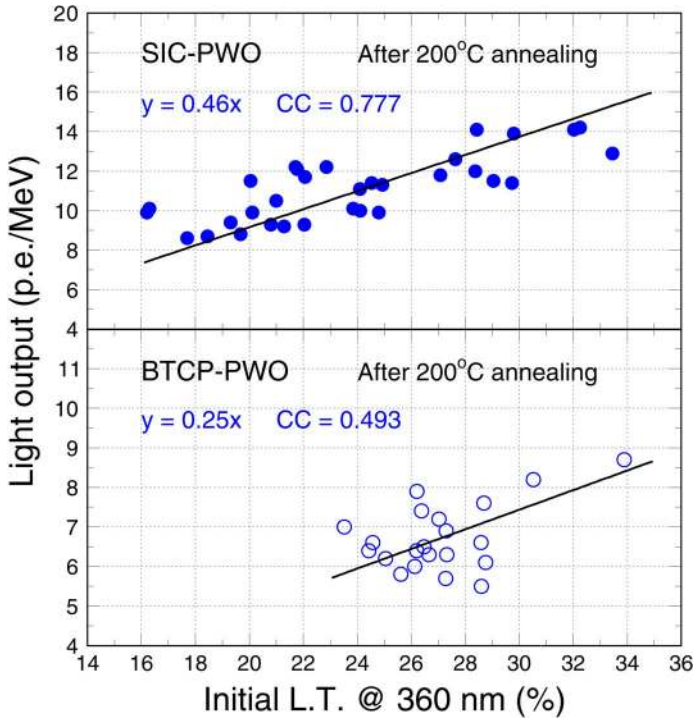


Fig. 9. Correlations between the initial light output versus the initial longitudinal transmittance at 360 nm for all SIC (top) and BTCP (bottom) samples.

at 360 nm. Also shown in these figures are the linear fits and corresponding linear correlation coefficients (CC), defined as

$$CC = \frac{\sum_{i=1}^{n}[(x_i - \bar{x})(y_i - \bar{y})]}{\sqrt{\sum_{i=1}^{n}(x_i - \bar{x})^2 \sum_{i=1}^{n}(y_i - \bar{y})^2}}. \quad (10)$$

We note that the BTCP samples have a higher longitudinal transmittance values at 360 nm as compared to the SIC samples. This is partly due to the fact that the BTCP samples were grown along the "$a$" axis, while SIC crystals along the "$c$" axis. The lanthanum doping in the BTCP samples also enhances the optical transmittance around the band edge [15]. The drawback of an excessive lanthanum doping in $PbWO_4$ crystals is a relative low light output as shown in Fig. 9 The linear fit also shows different slopes for the SIC and BTCP samples, which may be caused by their different crystal orientations. This observed correlation may partly be attributed to the self-absorption of the very blue part of the emission spectrum, as evidenced by the cross-over of the transmittance and emission spectra at 360 nm as shown in Fig. 10. This correlation was also observed by others [16].

### B. EWRIAC Versus Relative Losses of the Longitudinal Transmittance At 440 Nm

Fig. 11 shows correlations between the EWRIAC and the relative losses of the longitudinal transmittance at 440 nm. Strong linear correlations ($CC > 98\%$) were observed for all samples in the equilibrium at 15 rad/h (top left plot), 400 rad/h (top right plot) and 9 000 rad/h (bottom left plot) irradiations. The combined data (right bottom plot) fit well with a second order polynomial for all samples, indicating that the longitudinal transmittance at 440 nm is a good measure of the radiation damage. This result is consistent with our previous investigation where 440 nm was chosen for the monitoring wavelength because of its best linearity [13].

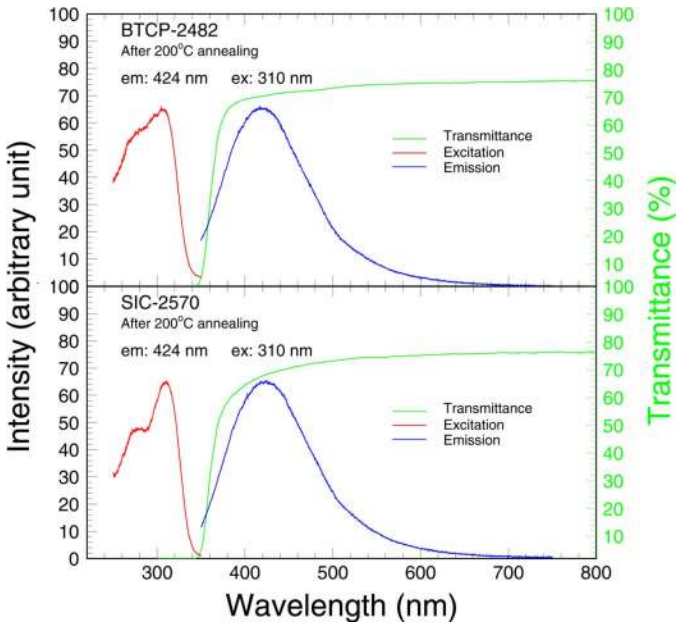


Fig. 10. The initial excitation (dotted lines, left scale), emission (solid line, left scale) and longitudinal transmittance (dot-dashed lines, right scale) are shown as a function as wavelength for the samples BTCP-2482 (top) and SIC-2570 (bottom).

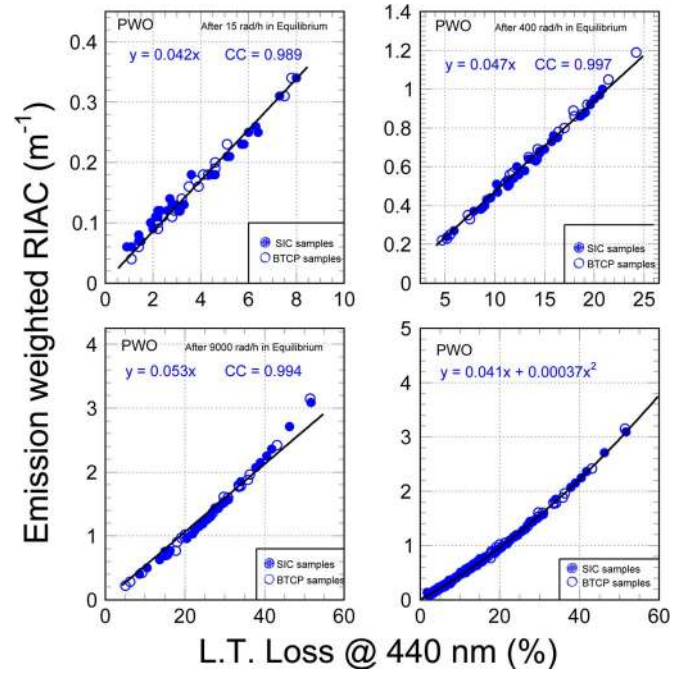


Fig. 11 Correlationsbetween the EWRIAC values and the relative losses of the longitudinal transmittance at 440 nm for all BTCP and SIC samples in the equilibrium under irradiations of different dose rates.

### *C. Relative Losses of the Light Output Versus That of the Longitudinal Transmittance At 440 Nm and the EWRIAC*

Fig. 12 shows correlations between the relative losses of the light output versus the relative losses of the longitudinal transmittance at 440 nm (top plot) and the corresponding EWRIAC values (bottom plot) for all samples in the equilibrium under 15 rad/h irradiations. Positive correlations are observed with the linear correlation coefficient at 50% level.

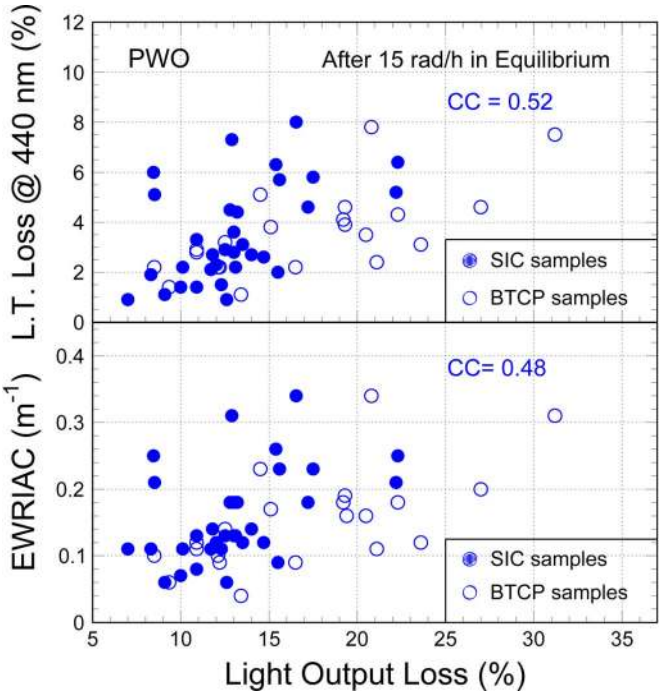


Fig. 12. Correlations between the relative losses of the longitudinal transmittance at 440 nm (top) and the EWRIAC values (bottom) versus the relative losses of the light output for all BTCP and SIC samples in the equilibrium under 15 rad/h irradiations.

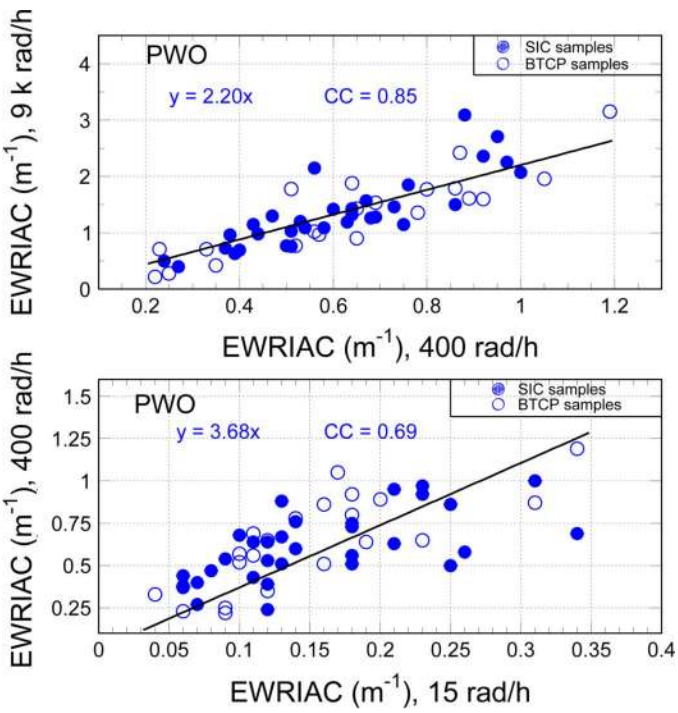


Fig. 13. Correlations between the EWRIAC values measured for all BTCP and SIC samples in the equilibrium under irradiations of different dose rates.

### *D. EWRIAC Values in the Equilibrium At Different Dose Rates*

The top plot of Fig. 13 shows correlations between the EWRIAC values measured for all samples in the equilibrium at 9 000 rad/h and 400 rad/h. The linear correlation coefficient is 85%, which is larger than 69% observed between 400 rad/h and 15 rad/h (bottom plot). The relatively weak correlations

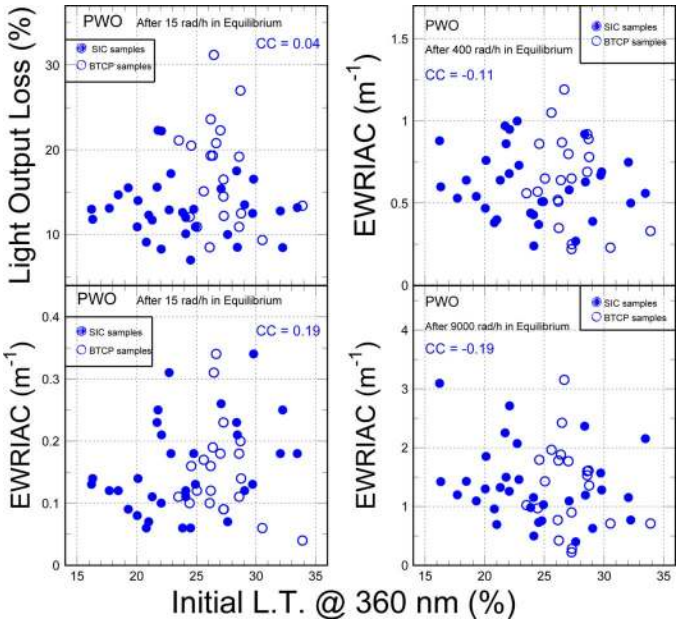


Fig. 14. Correlations between radiation damage (relative light output losses and the EWRIAC values) in the equilibrium under 15 rad/h irradiations and the initial longitudinal transmittance values at 360 nm for all BTCP and SIC samples.

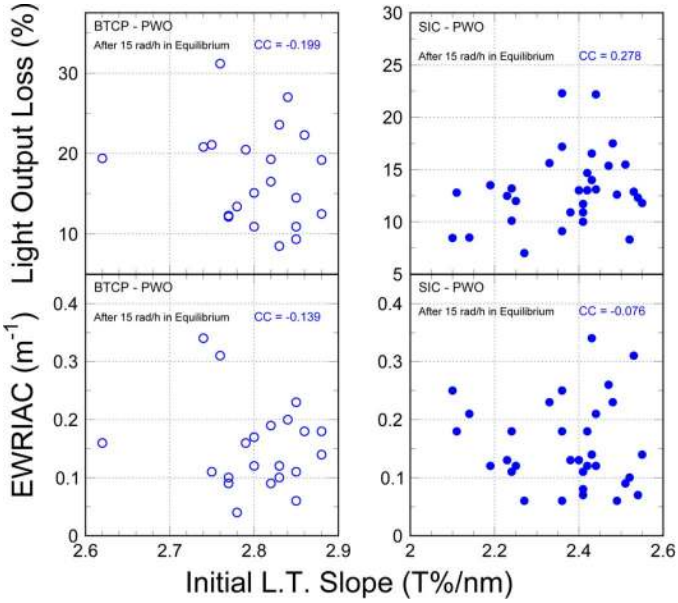


Fig. 15. Correlations between radiation damage (relative light output losses and the EWRIAC values) in the equilibrium under 15 rad/h irradiations and the initial longitudinal transmittance slopes across the band edge for all BTCP and SIC samples.

observed between low dose rates are a consequence of the preexisting absorptions, which is negligible for severe damages. The strong correlation observed between damages at high dose rates allows transferring, or comparing, the radiation damage data measured at different laboratories at different irradiation conditions. This correlation was also observed by others [16].

### *E. Radiation Damage Versus Initial Longitudinal Transmittance At 360 Nm*

We observed no correlations between crystal's radiation damage and its initial longitudinal transmittance. Fig. 14 shows correlations between various radiation damage measures and the values of the initial longitudinal transmittance at 360 nm for all samples. The corresponding linear correlation coefficients are 4%, 19%, −11% and −19% respectively for the relative losses of the light output at 15 rad/h (top left plot) and the EWRIAC values at 15 rad/h (bottom left plot), 400 rad/h (top right plot) and 9 000 rad/h (bottom right plot). Observations were the same for the initial longitudinal transmittance at difference wavelengths. This observation indicates that crystal's radiation induced color centers are not related to its preexisting absorption.

### *F. Radiation Damage Versus Initial Longitudinal Transmittance Slope Across the Band Edge*

We observed also no correlations between crystal's radiation damage and the slope values of its initial longitudinal transmittance across crystal's band edge. Fig. 15 shows the correlations between the slope values and the relative losses of the light output (top plots) and the corresponding EWRIAC (bottom plots) for all BTCP (left plots) and SIC (right plots) samples in the equilibrium at 15 rad/h irradiations. The linear correlation

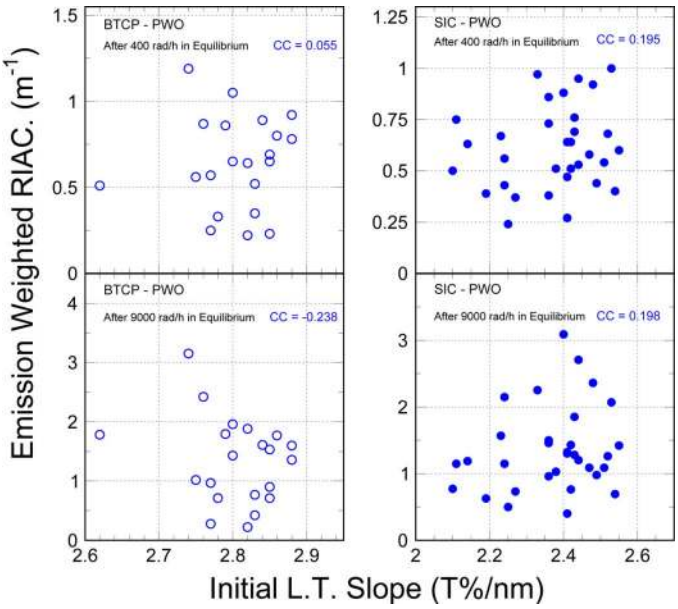


Fig. 16. Correlations between the EWRIAC values measured in the equilibrium under 400 and 9 000 rad/h irradiations and the initial longitudinal transmittance slopes across the band edge for all BTCP and SIC samples.

coefficients values are in the range of −20% to −14% for the BTCP samples and −8% to 28% for the SIC samples. Fig. 16 shows correlations between the slopes and the EWRIAC values measured for the BTCP (left plots) and SIC (right plots) samples in the equilibrium at high dose rates: 400 rad/h (top plots) and 9 000 rad/h (bottom plots). The corresponding linear correlation coefficient values are from −24% to 6% for the BTCP samples and about 20% for the SIC samples. A cross check by varying the wavelength range for the linear fit yields similar result. This result can be compared with an early observation [17], where a

very minor negative correlation was observed between the radiation hardness and the slope of the longitudinal transmittance across the band edge for some BTCP samples.

## IV. Summary

By using 53 $PbWO_4$ samples, a correlation was observed between crystal's initial longitudinal transmittance at 360 nm and its initial light output. A strong correlation was observed between the relative losses of the longitudinal transmittance at 440 nm and EWRIAC, which follows a universal $2^{nd}$ order polynomial for all samples. Correlations were also observed between the relative losses of $PbWO_4$ crystal's light output and the relative loses of its longitudinal transmittance at 440 nm or EWRIAC, indicating that the variation of the longitudinal transmittance 440 nm is a good measure of the radiation damage.

A correlation between the EWRIAC values measured at different dose rates was observed, which was relatively weak at low dose rates, where the consequence of the preexisting absorption is not negligible. This correlation has a practical application. One may measure crystals at a particular dose rate and predict its performance at different dose rates.

No correlations were observed between crystal's radiation hardness and its initial longitudinal transmittance, indicating that the radiation induced color centers are not intrinsically related to the preexisting absorptions. No correlations were observed between crystal's radiation hardness and the slopes of its initial longitudinal transmittance across the band edge for either BTCP or SIC samples. We conclude that predictions of $PbWO_4$ crystal's radiation hardness by using its initial optical properties are not reliable.

## Acknowledgment

The authors would like to thank the CMS ECAL Collaboration for providing all BTCP samples and 11 SIC samples used in this work. They would also like to thank Prof. J. Y. Liao, D. Z. Shen, and Z. W. Yin for providing 20 samples from SIC. Useful discussions with CMS and SIC colleagues are also acknowledged.

## References

[1] X. D. Qu, L. Y. Zhang, R.-Y. Zhu, J. Y. Liao, D. Z. Shen, and Z. W. Yin, "A study on yttrium doping in lead tungstate crystals," *Nucl. Instrum. Methods. Phys. Res. A* , vol. A480, pp. 470–487, 2002.

[2] E. Auffray, S. Balog, E. Bouquerel, P. Lecoq, M. Schneegans, and P. Sempere, "Status of the PWO crystal production for the electromagnetic calorimeter of CMS and its construction," *Nucl. Instrum. Methods. Phys. Res. A*, vol. A537, pp. 373–378, 2005.

[3] A. Gasparian, "Performance of PWO crystal detectors for a high resolution hybrid electromagnetic calorimeter at Jefferson lab," in *Proc. 10th Int. Conf. Calorimetry in Particle Physics*, R. Y. Zhu, Ed., 2002, pp. 208–214, PrimEx Collaboration, World Scientific.

[4] R. H. Mao, L. Y. Zhang, and R.-Y. Zhu, "Quality of mass produced lead tungstate crystals," *IEEE Trans. Nucl. Sci.*, vol. 51, no. 4, pp. 1777–1783, Aug. 2004.

[5] R. Y. Zhu, A Study on the Type III PWO Samples a talk in a CMS week, Dec 2003 [Online]. Available: http://www.hep.caltech.edu/~zhu/talks/ryz_031209_pwo.pdf

[6] R. Y. Zhu, D. A. Ma, H. B. Newman, C. L. Woody, J. A. Kierstead, and S. B. Paul, "A study on properties of lead tungstate crystals," *Nucl. Instrum. Methods Phys. Res. A*, vol. A376, pp. 319–334, 1996.

[7] R. Y. Zhu, Q. Deng, H. Newman, C. L. Woody, J. A. Kierstead, and S. B. Paul, "A study on radiation hardness of lead tungstate crystals," *IEEE Trans. Nucl. Sci.*, vol. 45, no. 3, pp. 686–691, Jun. 1998.

[8] R. Y. Zhu, "Radiation damage in scintillating crystals," *Nucl. Instrum. Methods Phys. Res. A*, vol. A413, pp. 297–311, 1998.

[9] R. Y. Zhu, Long Term Recovery of Seven PWO Crystals, Jul. 2003 [Online]. Available: http://www.hep.caltech.edu/~zhu/talks/ryz_030708_pwo.pdf

[10] D. A. Ma and R. Y. Zhu, "Light attenuation length of barium fluoride crystals," *Nucl. Instrum. Methods Phys. Res. A*, vol. A333, pp. 422–424, 1993.

[11] G. F. Bakhshieva and A. M. Morozov, "Refractive-Indexes of molybdate and tungstate single-crystals having scheelite structure," *Sov. J. Opt. Technol.*, vol. 44, no. 9, pp. 542–543, 1977.

[12] S. Baccaro, "Ordinary and extraordinary complex refractive index of the lead tungstate crystals," *Nucl. Instrum. Methods Phys. Res. A*, vol. A385, pp. 209–214, 2007.

[13] X. D. Qu, L. Y. Zhang, and R.-Y. Zhu, "Radiation induced color centers and light monitoring for lead tungstate crystals," *IEEE Trans. Nucl. Sci.*, vol. 47, no. 6, pp. 1741–1747, Dec. 2000.

[14] R. Y. Zhu, Result of Long Term Damage/Recovery Tests and Correlation Studies, Nov. 3, 2005 [Online]. Available: http://www.hep.caltech.edu/~zhu/talks/ryz_051103_pwo.pdf

[15] M. Kobayashi, "Improvement in transmittance and decay time of $PbWO_4$ scintillating crystals by La-doping," *Nucl. Instrum. Methods Phys. Res. A*, vol. A399, pp. 261–267, 1997.

[16] L. M. Barone, "Precision measurements of light yield and transmittance of lead tungstate crystals at the INFN-ENEA regional center," *Nucl. Instrum. Methods Phys. Res. A*, vol. A562, pp. 76–84, 2007.

[17] E. Auffray, M. Lebeau, P. Lecoq, and M. Schneegans, "Specifications for lead tungstate crystals preproduction," *CMS NOTE 98-038*, 1998.